

Synthesis, structures and electrochemical properties of ruthenium (II) complexes bearing bidentate 1,8-naphthyridine and terpyridine analogous (N,N,C)-tridentate ligands

Take-aki Koizumi, Takashi Tomon, Koji Tanaka *

Institute for Molecular Science and CREST, Japan Science and Technology Agency (JST), 5-1 Higashiyama, Myodaiji, Okazaki, Aichi 444-8787, Japan

Received 26 April 2005; received in revised form 18 June 2005; accepted 29 June 2005
Available online 8 August 2005

Abstract

1,8-Naphthyridine (napy) and terpyridine-analogous (N,N,C) tridentate ligands coordinated ruthenium (II) complexes, $[\text{RuL}(\text{napy-}\kappa^2\text{N,N}')(\text{dmsO})](\text{PF}_6)_2$ (**1**: $\text{L}=\text{L}^1=\text{N}''\text{-methyl-4'-methylthio-2,2':6',4''-terpyridinium}$, **2**: $\text{L}=\text{L}^2=\text{N}''\text{-methyl-4'-methylthio-2,2':6',3''-terpyridinium}$) were prepared and their chemical and electrochemical properties were characterized. The structure of complex **1** was determined by X-ray crystallographic study, showing that it has a distorted octahedral coordination style. The cyclic voltammogram of **1** in DMF exhibited two reversible ligand-localized redox couples. On the other hand, the CV of **2** shows two irreversible cathodic peaks, due to the Ru–C bond of **2** containing the carbenic character. The IR spectra of **1** in CO_2 -saturated CH_3CN showed the formation of Ru-($\eta^1\text{-CO}_2$) and Ru–CO complexes under the controlled potential electrolysis of the solution at -1.44 V (vs. Fc/Fc^+). The electrochemical reduction of CO_2 catalyzed by **1** at -1.54 V (vs. Fc/Fc^+) in DMF-0.1 M Me_4NBF_4 produced CO with a small amount of HCO_2H .

© 2005 Elsevier B.V. All rights reserved.

Keywords: Ruthenium; IR spectroscopy; CO_2 reduction; Electrochemistry; N,N,C ligands

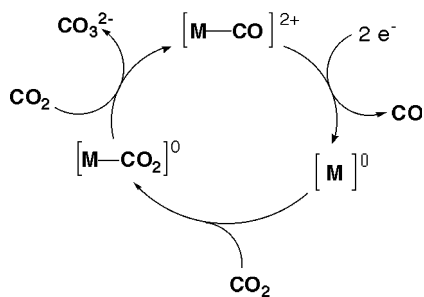
1. Introduction

Ruthenium complexes bearing polypyridyl ligand (2,2'-bipyridine (bpy), 2,2':6',2''-terpyridine (terpy), etc.) have attracted increasing attention as a catalyst for the photo- and electrochemical reactions [1]. Some of polypyridyl(carbonyl)ruthenium complexes work as homogeneous catalysts in the electrochemical reduction of carbon dioxide [2], where ligand localized redox reactions work as electron receivers in the reactions. Introduction of the metal–carbon σ -bond in the Ru-polypyridyl moiety would induce substantial changes

of the electron density of the metal center and the redox potential of the complexes compared with those of Ru-polypyridyl ones [3–10]. Along the line, we have examined the redox behavior of ruthenium complexes bearing terpy-analogous (N,N,C)-tridentate ligands containing a quaternized framework [10]. To our knowledge, there have not been investigated the electrochemical reduction of CO_2 by using the complexes containing these (N,N,C) or (N,C,N) tridentate ligands. Scheme 1 shows the proposed reduction mechanism of the electrochemical reduction of carbon dioxide catalyzed by a ruthenium carbonyl complex bearing polypyridyl ligands in aprotic solvents. When the Ru–CO complex receives two electrons, the Ru–CO bond becomes labile and penta-coordinated-electron rich intermediate is produced. In the presence of carbon dioxide, which is a kind of Lewis

* Corresponding author. Tel.: +81 564 59 5580; fax: +81 564 59 5582.

E-mail address: ktanaka@ims.ac.jp (K. Tanaka).



Scheme 1.

acid, the empty coordination site is occupied by CO_2 to give an $\text{Ru}-(\eta^1\text{-CO}_2)$ intermediate, followed by the disproportionation with another CO_2 molecule to reproduce the Ru-CO complex with production of CO_3^{2-} . If $\text{Ru}-(\eta^1\text{-CO}_2)$ and Ru-CO complexes (or their one- or two electron reduced products) that are intermediates of the electrochemical CO_2 reduction can be observed under the electrochemical reduction atmosphere, they can become strong evidences for the above-mentioned reaction mechanism correctness. However, there have been few examples for observations of the coordination process of CO_2 to the metal center and the transformation process of CO_2 to CO by spectroscopic methods [11], in particular, to our knowledge, no report for ruthenium complexes. In this study, we have prepared ruthenium complexes bearing 1,8-naphthyridine (napy) and a quaternized (N,N,C)-tridentate ligand to elucidate the catalytic activity toward the reduction of carbon dioxide. Napy gives rise to the exchange of coordination mode between monodentate and bidentate easily, thus the complex containing chelated napy could smoothly provide the coordination site for CO_2 when the complex is reduced. We have succeeded the observation of the $\text{Ru}-(\eta^1\text{-CO}_2)$ and Ru-CO complexes as intermediates of electrochemical CO_2 reduction by infrared spectroscopic studies under controlled potential electrolysis conditions in CO_2 -saturated MeCN, and have demonstrated the electrochemical reduction of CO_2 by using the ruthenium complex as a catalyst precursor.

2. Experimental

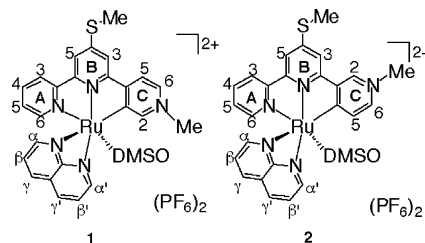
2.1. General, measurement, and materials

^1H , $^{13}\text{C}\{^1\text{H}\}$, and $^1\text{H}-^1\text{H}$ COSY NMR spectra were recorded on a JEOL GX-500 spectrometer. IR spectra were recorded on a Shimadzu-FTIR 8100 spectrophotometer. Electronic spectra were collected on a Shimadzu UV-3100PC UV-Vis-NIR scanning spectrometer. ESI-MS spectra were obtained on a Shimadzu LCMS-2010 spectrometer. Electrochemical measurements were performed with ALS/chi Electrochemical Analyzer 660A. A conventional three-electrode configuration was used,

with a glassy carbon working (BAS PFCE carbon electrode) and a platinum wire auxiliary electrode (BAS special order) and an Ag/Ag^+ reference (BAS RE-5). Cyclic voltammograms were recorded at a scan rate of 100 mV s^{-1} . Electrochemical reduction of CO_2 was performed in CO_2 -saturated DMF containing a ruthenium complex ($1.0 \times 10^{-3} \text{ mol L}^{-1}$), Me_4NBF_4 (0.1 mol L^{-1}) as a supporting electrolyte, and $[\text{Ru}(\text{bpy})_3](\text{PF}_6)_2$ ($1.0 \times 10^{-2} \text{ mol L}^{-1}$) as an electron carrier under controlled potential electrolysis at -1.45 to -1.60 V (vs. Fc/Fc^+). The electrolysis cell consisted of a glassy carbon working electrode, a magnesium ribbon auxiliary electrode, and an Ag/AgNO_3 0.1 M reference electrode. The electrolysis was performed with a Hokuto Denko HA-501 potentiostat, and the electricity consumed was measured with a Hokuto Denko HF-201 Coulomb meter. Carbon dioxide evolved in the gaseous phase was analyzed by a Shimadzu GC-8A gas chromatograph equipped with a 2 m column filled with Molecular Sieve 13X at 40°C using He as the carrier gas. The amount of HCO_2H produced in the reduction was measured by a Shimadzu IP-3A isotachopheric analyzer. Elemental analyses were carried out by the Molecular Scale Nano-Science Center of IMS. $(\text{L}^1\text{H})(\text{PF}_6)$ [10a], $(\text{L}^2\text{H})(\text{PF}_6)$ [10a], and $\text{RuCl}_2(\text{napy-}\kappa^2\text{N,N}')(\text{dms})_2$ [10b] were prepared according to the literature method. Solution IR spectra under electrolysis conditions were obtained by using a KBr cell equipped with a spacer made of Novix Films (purchased from Iwaki Co. Ltd.), an Au mesh for a working electrode, a Pt wire for an auxiliary electrode, and a luggin capillary to separate a reference electrode from the working electrode. The thickness of the cell was 0.3 mm , and the total cell volume was 0.1 cm^3 . A CH_3CN or CD_3CN solution containing a metal complex ($1 \times 10^{-2} \text{ mol L}^{-1}$) and Me_4NBF_4 ($5 \times 10^{-2} \text{ mol L}^{-1}$) in the IR cell was exposed to an IR ray only on measuring to prevent the evaporation of CO_2 from the solution. The numbering of aromatic protons of **1** and **2** is shown in Scheme 2.

2.2. preparation of $[\text{RuL}^1(\text{napy-}\kappa^2\text{N,N}')(\text{dms})](\text{PF}_6)_2$ (**1**)

To a $\text{CH}_3\text{OCH}_2\text{CH}_2\text{OH}$ solution (20 mL) of $\text{RuCl}_2(\text{napy-}\kappa^2\text{N,N}')(\text{dms})_2$ (100 mg, 0.218 mmol) was added a $\text{CH}_3\text{OCH}_2\text{CH}_2\text{OH}$ solution (5 mL) of AgPF_6



Scheme 2.

(110 mg, 0.436 mmol) and stirred at 60 °C for 1 h. The resulting off-white solid was eliminated by celite filtration, and then the orange filtrate was added to a CH₃OCH₂CH₂OH solution (5 mL) of (L¹H)(PF₆) (96 mg, 0.218 mmol). The reaction mixture was stirred at 70 °C, the color turned immediately from orange to dark brown. After 24 h, the solution was concentrated to ca. 1 mL, and poured into an aqueous NH₄PF₆ solution. The resulting dark brown solid was collected by filtration and dried in vacuo, and recrystallized from acetone–ethanol to give **1** as brownish purple crystals (165 mg, 85%). ESI-MS: $m/z = 301\{M - 2PF_6\}^{2+}$. Anal. Calcd for C₂₇H₂₇F₁₂N₅OP₂RuS₂: C, 36.33; H, 3.05; N, 7.85. Found C, 37.00; H, 3.50; N, 7.51. ¹H NMR (500 MHz in acetone-*d*₆): δ 9.64 (d, 1H, H^α, $J(H-H) = 4.3$ Hz), 8.81 (d, 1H, H^{3A}, $J(H-H) = 7.9$ Hz), 8.78 (d, 1H, H^{6A}, $J(H-H) = 7.9$ Hz), 8.76 (d, 1H, H^γ, $J(H-H) = 10.4$ Hz), 8.68 (d, 1H, H^α, $J(H-H) = 8.5$ Hz), 8.55 (d, 1H, H^{5C}, $J(H-H) = 6.7$ Hz), 8.55 (s, 1H, H^{2C}), 8.53 (d, 1H, H^{6C}, $J(H-H) = 6.7$ Hz), 8.49 (s, 1H, H^{3B}), 8.47 (s, 1H, H^{5B}), 8.46 (d, 1H, H^γ, $J(H-H) = 7.9$ Hz), 8.28 (t, 1H, H^{4A}, $J(H-H) = 7.3$ Hz), 8.03 (dd, 1H, H^β, $J(H-H) = 8.6$ and 4.9 Hz), 7.71 (t, 1H, H^{5A}, $J(H-H) = 6.7$ Hz), 7.56 (dd, 1H, H^β, $J(H-H) = 8.6$ and 4.9 Hz), 4.21 (s, 3H, N-Me), 2.87 (s, 3H, S-Me), 2.62 (s, 3H, DMSO), 2.59 (s, 3H, DMSO). ¹³C{¹H} NMR (125 MHz in acetone-*d*₆): δ 179.3 (Ru-C), 165.0, 161.8, 158.4, 157.7, 157.2, 156.3, 154.1, 153.9, 152.9, 151.1, 139.8, 139.7, 138.5, 136.6, 129.0, 126.7, 125.8, 124.8, 120.8, 120.6, 119.8, 119.6, 47.8, 45.6, 45.0, 14.6. UV-Vis (acetone): λ_{max}/nm (ε/dm³ mol⁻¹ cm⁻¹) 425.5 (8830).

2.3. Preparation of [RuL²(napy-κ²N,N')(dmsO)](PF₆)₂ (**2**)

To a CH₃OCH₂CH₂OH solution (20 mL) of RuCl₂(napy-κ²N,N')(dmsO)₂ (100 mg, 0.218 mmol) was added a CH₃OCH₂CH₂OH solution (5 mL) of AgPF₆ (110 mg, 0.436 mmol) and stirred at 60 °C for 1 h. The resulting off-white solid was eliminated by celite filtration, and then the orange filtrate was added to a CH₃OCH₂CH₂OH solution (5 mL) of (L²H)(PF₆) (96 mg, 0.218 mmol). The reaction mixture was stirred at 70 °C, the color turned immediately from orange to dark brown. After 24 h, the solution was concentrated to ca. 1 mL, and poured into an aqueous NH₄PF₆ solution. The resulting reddish brown solid was collected by filtration and dried in vacuo, and recrystallized from acetone–ethanol to give **2** as reddish brown crystals (156 mg, 80%). ESI-MS: $m/z = 301\{M - 2PF_6\}^{2+}$. Anal. Calc. for C₂₇H₂₇F₁₂N₅OP₂RuS₂: C, 36.33; H, 3.05; N, 7.85. Found C, 36.08; H, 3.27; N, 7.70%. ¹H NMR (270 MHz in acetone-*d*₆): δ 9.66 (dd, 1H, H^α, $J(H-H) = 4.9$ and 1.2 Hz), 9.09 (s, 1H, H^{2C}), 8.90 (dd, 1H, H^{3A}, $J(H-H) = 4.9$ and 1.2 Hz), 8.81 (d, 1H, H^{6A}, $J(H-H) = 9.2$ Hz), 8.79 (dd, 1H, H^γ, $J(H-H) = 8.5$ and 1.2

Hz), 8.71 (dd, 1H, H^γ, $J(H-H) = 8.5$ and 1.2 Hz), 8.47 (dd, 1H, H^α, $J(H-H) = 4.3$ and 1.8 Hz), 8.44 (d, 1H, H^{3B}, $J(H-H) = 1.8$ Hz), 8.30 (d, 1H, H^{5B}, $J(H-H) = 1.2$ Hz), 8.29 (dt, 1H, H^{4A}, $J(H-H) = 7.9$ and 1.8 Hz), 8.07 (dd, 1H, H^β, $J(H-H) = 8.5$ and 4.9 Hz), 8.00 (dd, 1H, H^{6C}, $J(H-H) = 6.1$ and 1.2 Hz), 7.93 (d, 1H, H^{5C}, $J(H-H) = 6.1$ Hz), 7.72 (ddd, 1H, H^{5A}, $J(H-H) = 7.3$, 5.5, and 1.2 Hz), 7.59 (dd, 1H, H^β, $J(H-H) = 8.5$ and 4.9 Hz), 4.27 (s, 3H, N-Me), 2.84 (s, 3H, S-Me), 2.63 (s, 3H, DMSO), 2.59 (s, 3H, DMSO). ¹³C{¹H} NMR (125 MHz in acetone-*d*₆): δ 219.8 (Ru-C), 160.2, 157.1, 155.6, 155.5, 154.7, 152.8, 152.7, 151.9, 149.1, 138.9, 137.5, 137.1, 136.3, 135.6, 133.2, 127.6, 125.5, 124.6, 123.4, 119.6, 117.5, 115.5, 46.2, 44.3, 44.2, 13.8. UV-Vis (acetone): λ_{max}/nm (ε/dm³ mol⁻¹ cm⁻¹) 395.0 (7600).

2.4. Crystal structure determination

Crystals for X-ray analyses were obtained as described in the preparations. Suitable crystals were mounted on sealed in thin-walled glass capillaries. Data collection for **1** was performed at -100 °C on a Rigaku/MSM Mercury CCD diffractometer with graphite monochromated Mo Kα radiation (λ = 0.7107 Å). The structure was solved by using the teXsan software package. Atomic scattering factors were obtained from the literature [12]. Refinements were performed anisotropically for all non-hydrogen atoms by the full-matrix least-squares method. Hydrogen atoms were placed at the calculated positions and were included in the structure calculation without further refinement of the param-

Table 1
Crystal data and details of the structure refinement of **1**

Formula	C ₂₇ H ₂₇ F ₁₂ N ₅ OP ₂ RuS ₂
Molecular weight	892.66
Crystal system	Triclinic
Space group	<i>P</i> $\bar{1}$ (no. 2)
<i>a</i> (Å)	8.901(5)
<i>b</i> (Å)	12.039(7)
<i>c</i> (Å)	17.786(9)
α (°)	105.710(5)
β (°)	92.379(6)
γ (°)	106.869(8)
<i>V</i> (Å ³)	1814(1)
<i>Z</i>	2
μ (cm ⁻¹)	7.27
<i>F</i> (000)	892.00
<i>D</i> _{calcd} (g cm ⁻³)	1.633
Number of unique reflections	7875
Number of reflections used	7781
Number of variables	451
<i>R</i> ₁	0.085
<i>R</i>	0.099
<i>R</i> _w	0.119

$$R_1 = \frac{\sum |F_o| - |F_c|}{\sum |F_o|} \text{ for } I > 2.0\sigma(I) \text{ data, } R_w = \frac{\sum [\omega(F_o^2 - F_c^2)^2]}{\sum \omega(F_o^2)^2}]^{1/2} \text{ weighting scheme } [1/\sum (F_o)^2]^{1/2}.$$

ters. The residual electron densities were of no chemical significance. Crystal data and processing parameters are summarized in Table 1.

3. Results and discussion

Complexes **1** and **2** with (N,N,C)-tridentate ligand **L**¹ or **L**² were prepared as shown in Scheme 3. Treatment of RuCl₂(napy-κ²N,N')(dmsO)₂ with 2 equiv. of AgPF₆ in 2-methoxyethanol resulted in the formation of an orange solution with AgCl precipitation. The Ag salt was removed by filtration, and then (L¹H)(PF₆) was added to the filtrate to give a dark brown solution. The resulting solution was concentrated, and poured into an aqueous NH₄PF₆ solution to give **1** in 85% yield. Similarly, an addition of (L²H)(PF₆) to the orange solution, instead of (L¹H)(PF₆), gave the complex **2** in 80% yield. In each case, the cyclometalation took place smoothly. ESI-MS spectra of **1** and **2** showed the parent peak of [RuL(napy-κ²N,N')(dmsO)]²⁺ at *m/z* = 301. On the other hand, treatment of terpy in place of (L¹H)(PF₆) and (L²H)(PF₆) with the orange solution predominantly induced ligand disproportionation reactions. Because the ESI-MS spectrum showed that the product contained several complexes such as [Ru(terpy)₂]²⁺, [Ru(terpy)(napy)₂]²⁺ and so on, and the isolation of [Ru(terpy)(napy)(dmsO)]²⁺ was not succeed. This result indicated that (N,N,C)-tridentate ligands forbid the ligand disproportionation or redistribution of complexes due to the strong ligand field based on the metal–carbon bond.

Fig. 1 shows the molecular structure of **1** determined by X-ray crystallographic study. Complex **1** adopts a monomeric, distorted octahedral coordination around the Ru(II) center with one *S*-coordinated dimethylsulfoxide, one chelating napy and the (N,N,C)-tridentate ligand. The bond distances between ruthenium and the (N,N,C) ligand (Ru1–N1, 2.149(6) Å; Ru1–N2,

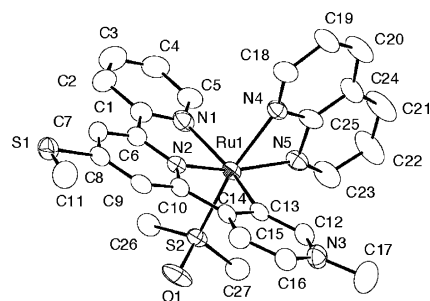
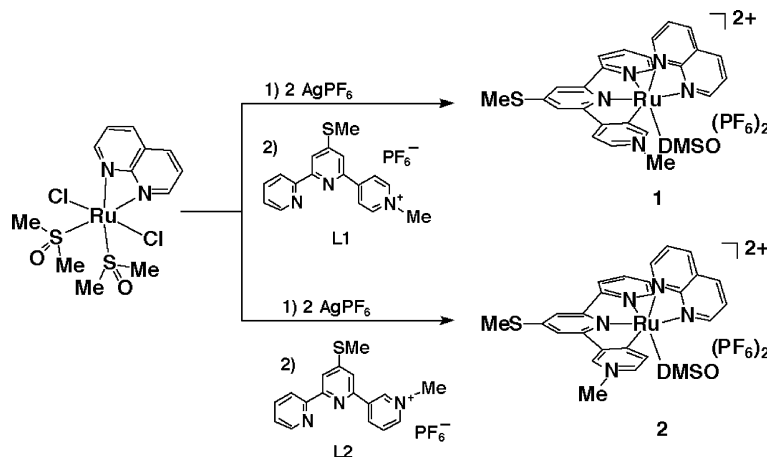


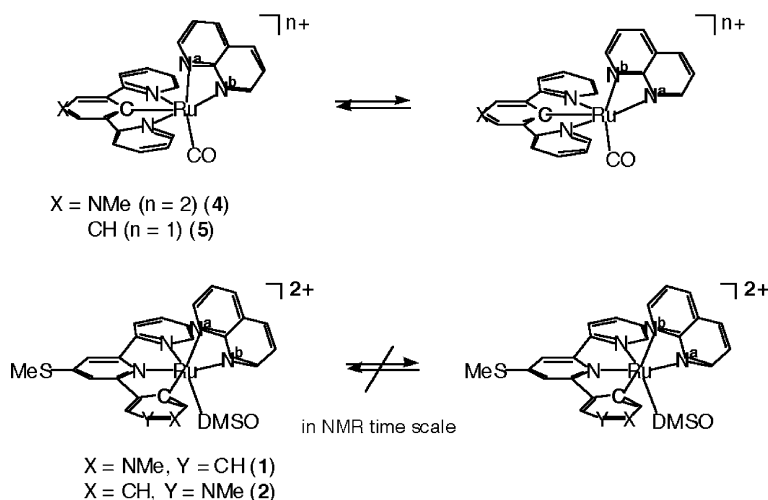
Fig. 1. ORTEP drawing of the cationic part of **1**. Hydrogen atoms are omitted for clarity. Selected bond distances (Å) and angles (°): Ru1–N1, 2.149(6); Ru1–N2, 2.002(5); Ru1–N4, 2.138(5); Ru1–N5, 2.138(6); Ru1–C13, 2.071(6); Ru1–S2, 2.221(2); N3–C17, 1.45(1); N1–Ru1–N2, 78.8(2); N1–Ru1–C13, 158.1(2); N1–Ru1–N4, 89.6(2); N1–Ru1–N5, 100.2(2); N1–Ru1–S2, 93.9(2); N2–Ru1–C13, 79.7(2); N2–Ru1–N4, 102.0(2); N2–Ru1–N5, 165.0(2); N2–Ru1–S2, 90.2(2); N4–Ru1–C13, 90.5(2); N4–Ru1–N5, 62.9(2); N4–Ru1–S2, 167.7(2); N5–Ru1–C13, 99.5(2); N5–Ru1–S2, 104.8(2); C13–Ru1–S2, 90.7(2); C8–S1–C11, 104.8(4).

2.002(5) Å; Ru1–C13, 2.071(6) Å) are in good accordance with previously reported Ru-(N,N,C) complexes [4b,10a]. The bond distances between ruthenium and two N atoms in the napy ligand are 2.138(5) Å (Ru1–N4) and 2.138(6) Å (Ru1–N5), respectively, indicating that the napy ligand coordinates symmetrically. The coordination state is different from previously reported chelated napy ligand in the (N,C,N) tridentate ligand-coordinating [RuL³(napy-κ²N,N')L']²⁺ (**L**³ = *N*-methyl-3,5-di(2-pyridyl)-4-pyridyl, **3**: L' = DMSO; **4**: L' = CO), which have an unsymmetrical coordination fashion [10b]. In addition, the average of the Ru–N bond lengths is similar to that of previously reported [Ru(napy-κ²N,N')(bpy)₂]²⁺, which has symmetrically coordinated napy (2.11(1) Å) [13], and shorter than those of **3** (2.215 Å) and **4** (2.200 Å) [10b].

¹H NMR spectra of **1** and **2** recorded in acetone-*d*₆ at room temperature display 15 resonances in aromatic region, which are assigned to one unsymmetrical napy and



Scheme 3.

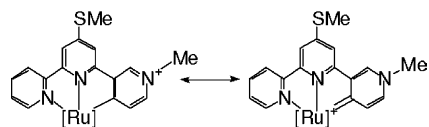


Scheme 4.

an (N,N,C)-ligand. Previously, we have reported the fluxional behavior of the napy ligand in Ru-(N,C,N)-complexes **4** and **5** ($[\text{RuL}^4(\text{napy}-\kappa^2\text{N},\text{N}')(\text{CO})]^+$, $\text{L}^4 = 2,6\text{-di}(2\text{-pyridyl})\text{phenyl}$) detected by ^1H NMR irradiation experiments [10b]. Those napy ligands rotate in the NMR time scale (Scheme 4). In contrast with those cases, the napy ligands in **1** and **2** did not show such fluxionality. The difference in fluxional behavior of these complexes would originate in the *trans* influence caused by the sort of ligands situated at *trans* positions of two N atoms of napy. This result indicates that the chelated napy ligand in **1** coordinates to ruthenium stronger than those of **4** and **5**, and is accordance with the result of X-ray determination as mentioned above [14].

In $^{13}\text{C}\{^1\text{H}\}$ NMR spectra, the signals for carbon of **1** and **2** which coordinate to the ruthenium center directly are observed at δ 179.3 and 219.8, respectively, being accordance with those of $[\text{RuL}^1(\text{terpy})](\text{PF}_6)_2$ and $[\text{RuL}^2(\text{terpy})](\text{PF}_6)_2$ [10a]. These results indicate that the quaternized pyridine unit in **1** has a pyridinium structure, and that in **2** has a pyridinylidene one (Scheme 5).

Electrochemical studies of **1** and **2** were performed in a DMF solution, and the results are collected in Table 2. Complex **1** exhibited two stepwise reversible couples based on the napy and (N,N,C)-tridentate ligand-localized reductions at $E_{1/2} = -1.28$ V and -1.46 V (vs. Fc/Fc^+) under N_2 , respectively (Fig. 2(a)). On the other hand, **2** showed two irreversible ligand-localized reduction waves at $E_{\text{pc}} = -1.36$ V and -1.76 V (vs. Fc/Fc^+ , Fig. 2(b)). The quaternized



Scheme 5.

Table 2
Electrochemical data for **1** and **2**

Species	$E_{1/2}$ V (vs. Fc/Fc^+)		
	Ru(II)/Ru(III)	$[\text{Ru}]^{2+}/[\text{Ru}]^+$	$[\text{Ru}]^+/\text{Ru}^0$
1	n.d.	-1.28	-1.46
2	n.d.	-1.36 (E_{pc} , irr)	-1.76 (E_{pc} , irr)

Electrolyte, 0.1 M Me_4NBF_4 .

position in the (N,N,C)-ligand also has a great effect on the redox potential of the complex [10a]. In a CO_2 -saturated DMF solution, strong catalytic currents at ca. -1.5 V for **1** and ca. -1.7 V for **2** were observed, respectively (Figs. 2(c) and (d)). These results strongly suggest that both **1** and **2** have an ability to reduce CO_2 , and **1** is expected to work as a CO_2 -reduction catalyst at potentials more positive than **2**. Therefore, we tried to detect the transformation of CO_2 to reduced products by in situ infrared monitoring using a thin-layer cell by using complex **1**. Fig. 3 shows in situ monitoring of spectroelectrochemical phenomena of **1** in CO_2 -saturated acetonitrile as the potential of working electrode changes. Before starting the reduction, there are no peaks assigned to $\nu(\text{C}\equiv\text{O})$ in the range of $1850\text{--}2050$ cm^{-1} . When the potential of the working electrode shifted to negative direction, the first reduction took place at ca. -1.20 V, and the second one occurred at ca. -1.35 V (vs. Fc/Fc^+). At -1.44 V, new bands grew into the spectrum at 1281, 1873, and 1942 cm^{-1} (Fig. 3(a)). The former one is assigned to $\nu_{\text{asym}}(\text{CO}_2)$ band of the $\eta^1\text{-CO}_2$ -coordinated complex, and latter two are considered to $\nu(\text{C}\equiv\text{O})$ bands of Ru-CO complex (vide infra). The $\nu(\text{C}\equiv\text{O})$ bands are observed at lower wavenumber than those of general Ru-CO complexes because of the reduced atmosphere. Next, the potential was changed to -0.95 V, the peak at 1280 cm^{-1} decreased, and the peaks at 1873 and 1942 cm^{-1} shifted to 1956 and 2027 cm^{-1} , respectively

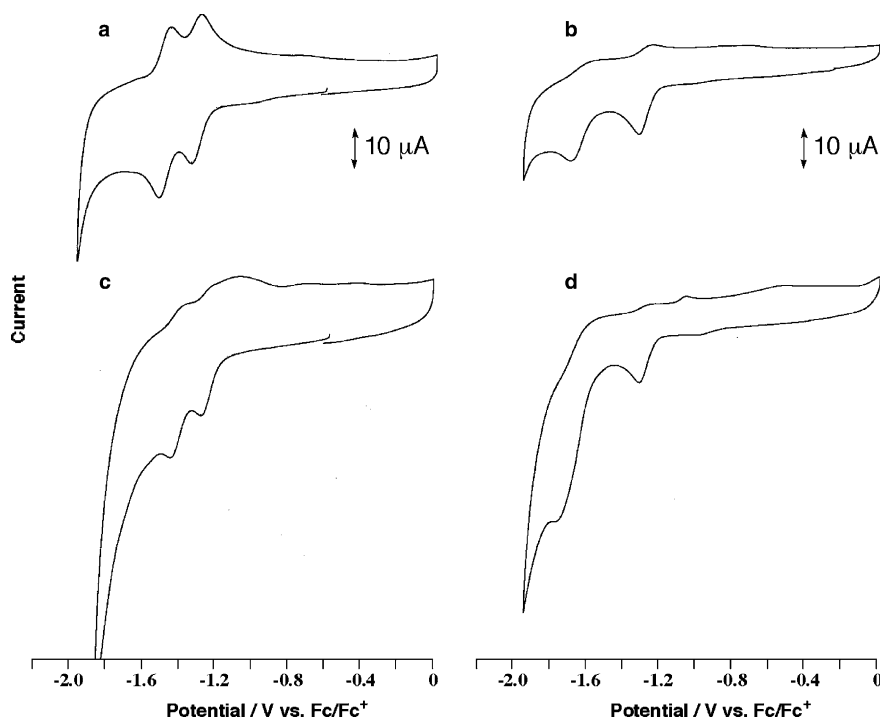


Fig. 2. Cyclic voltammograms of **1** and **2**: (a) **1** in DMF-N₂; (b) **2** in DMF-N₂; (c) **1** in DMF-CO₂, (d) **2** in DMF-CO₂.

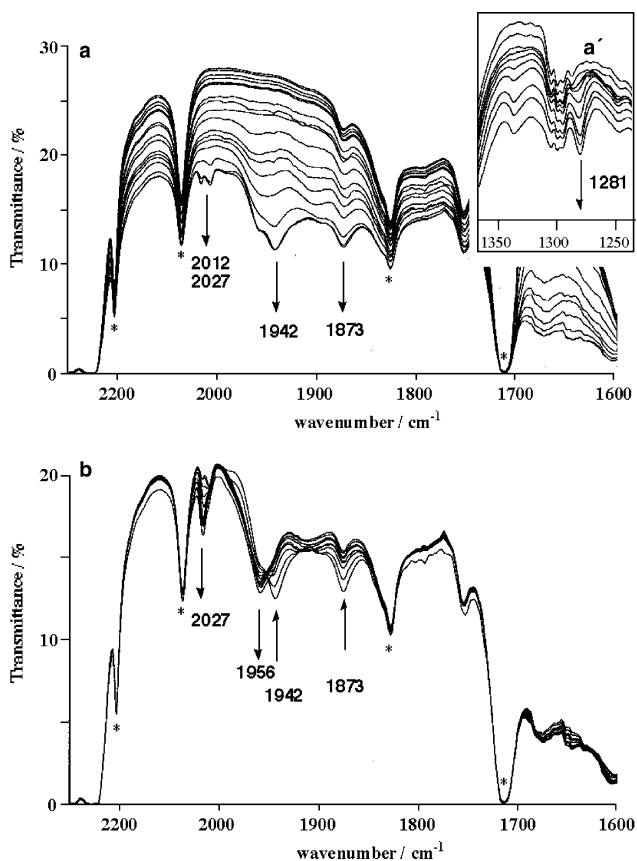
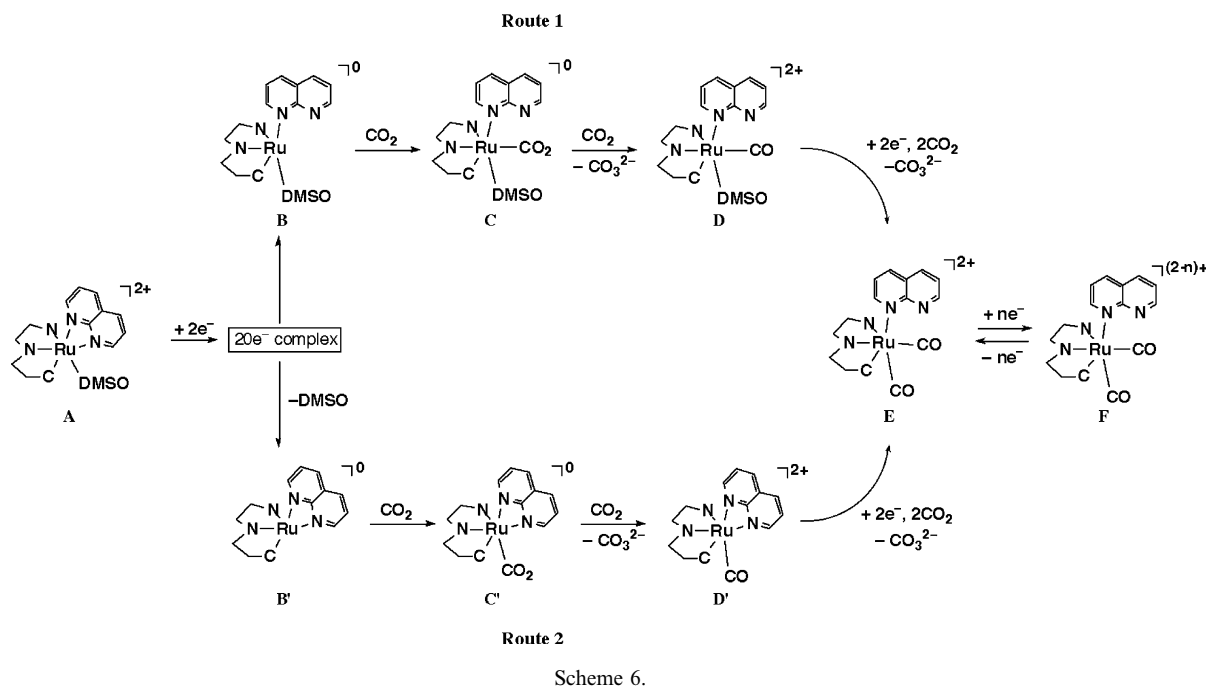


Fig. 3. IR spectra of [1](PF₆)₂ under the controlled potential electrolysis in CH₃CN ((a) and (b)) or CD₃CN (a'): (a) the potential was swept from -0.95 to -1.45 V; (b) the potential was swept from -1.45 to -0.95 V (vs. Fc/Fc⁺). * denotes CH₃CN peaks.

(Fig. 3(b)). Such the shifting of the $\nu(\text{C}\equiv\text{O})$ bands by electrochemical reduction-oxidation has been observed at other Ru-CO complexes [15], suggesting that these latter two absorption bands are assigned to $\nu(\text{C}\equiv\text{O})$. At -1.44 V, two relatively strong absorption bands assignable to two $\nu(\text{CO})$ ones were observed. This result indicates that species **E** [16] or **F** shown in Scheme 6 would be generated at the potential. The complex **A** receives two electrons to generate a 20 electron-species at -1.44 V (vs. Fc/Fc⁺). To keep the 18 electronic state, dechelation of chelated napy (**B**) or dissociation of DMSO (**B'**) would take place to give a penta-coordinate intermediate. CO₂ is a kind of Lewis acid, so it can attack the electron-rich ruthenium center of **B** or **B'** electrophilically, then the Ru-(η^1 -CO₂) intermediate **C** or **C'** would be generated. They can be converted into the Ru-CO complex (**D** or **D'**) with the formation of CO₃²⁻ by disproportionation with another CO₂ molecule as shown in Scheme 1. Further two-electron reduction of **D** and **D'** would lead to the formation of the dicarbonyl intermediate **E** through routes 1 and 2. The IR spectra shown in Fig. 3, therefore, are reasonably explained by the generation of the reduced form **E** in Scheme 6. The CV of **1** shows two reversible ligand-localized redox couples as mentioned above, indicating that dissociation of DMSO from Ru would not take place at -2.0 V. Thus, Route 1 may take priority over Route 2.

The catalytic activity of **1** for the electrochemical reduction of CO₂ was investigated. In the presence of CO₂, the cathodic current of two reduction waves



increased. The increase for the first reduction step is small whereas a strong increase for the second step can be observed, indicating that the two electron reduced species is the most active catalyst which transforms the CO_2 . Controlled-potential electrolysis of **1** at -1.55 V (vs. Fc/Fc^+) with a glassy carbon electrode in CO_2 -saturated DMF in the presence of Me_4NBF_4 produced CO with current efficiencies of 35% and with small amount of HCO_2H (2%) was formed at room temperature.

4. Conclusion

New ruthenium (II) complexes bearing chelated napy and (N,N,C) tridentate ligands have been synthesized and these electrochemical properties were investigated. Because of the formation of a metal–carbon bond, (N,N,C)-ligands do not cause the ligand-redistribution which is often observed in the reaction by using terpyridine-coordinated complexes. Cyclic voltammetric studies showed that the two-electron reduction of **2** took place at ca. 300 mV more negative than that of **1**, due to the difference of the coordination mode of the Ru–C bond. In the infrared spectroscopic study under controlled potential electrolysis conditions, the bands based on Ru(η^1 - CO_2) and Ru–CO complexes appeared under the electrolysis at -1.44 V (vs. Fc/Fc^+), where the complex receives two-electron reduction. This is the first example of the direct observation of the Ru–CO complex formation by the electrochemical reduction of CO-free ruthenium complexes in CO_2 -saturated solution. In addition, we have demonstrated

that complex **1** has an ability as a catalyst for CO_2 reduction electrochemically.

5. Supplementary materials

Crystallographic data for the structural analysis of **1** in CIF format has been deposited with the Cambridge Crystallographic Data Centre under CCDC No. 261152. These data can be obtained free of charge via www.ccdc.cam.ac.uk/conts/retrieving.html (or from the CCDC, 12 Union Road, Cambridge CB2 1EZ, UK; fax: +44 1223 336033; e-mail: deposit@ccdc.cam.ac.uk).

Acknowledgement

T.K. thanks Miss Kanako Tsutsui of our laboratory for measurements of electronic spectra.

References

- [1] Recent reviews of Ru(polypyridyl) complexes for photo- and electrochemistry, see; (a) V. Balzani, A. Julis, M. Venturi, S. Campagna, S. Serroni, *Chem. Rev.* 96 (1996) 759; (b) S. Norman, C. Carol, E. Fujita, *Comments Inorg. Chem.* 19 (1997) 67; (c) C.G. Garcia, J.F. de Lima, N.Y.M. Iha, *Coord. Chem. Rev.* 196 (2000) 219; (d) S. Fanni, T.E. Keyes, M. O'Connor, H. Hughes, R. Wang, J.G. Vos, *Coord. Chem. Rev.* 208 (2000) 77; (e) C.A. Kelly, G.J. Meyer, *Coord. Chem. Rev.* 211 (2001) 295.
- [2] (a) H. Ishida, K. Tanaka, T. Tanaka, *Organometallics* 6 (1987) 181;

- (b) M.R.M. Bruce, E. Megehee, B.P. Sullivan, H. Thorp, T.R. O'Toole, A. Downard, T.J. Meyer, *Organometallics* 7 (1988) 238;
- (c) J.R. Pugh, M.R.M. Bruce, B.P. Sullivan, T.J. Meyer, *Inorg. Chem.* 30 (1991) 86;
- (d) M.R.M. Bruce, E. Megehee, B.P. Sullivan, H. Thorp, T.R. O'Toole, A. Downard, J.R. Pugh, T.J. Meyer, *Inorg. Chem.* 31 (1992) 4864;
- (e) T. Yamamoto, T. Maruyama, Z.-H. Zhou, T. Ito, T. Fukuda, Y. Yoneda, F. Begam, T. Ikeda, S. Sasaki, H. Takezoe, A. Fukuda, K. Kubota, *J. Am. Chem. Soc.* 116 (1994) 4832;
- (f) M.N. Collomb-Dunand-Sauthier, A. Deronzier, R. Ziessel, *Inorg. Chem.* 33 (1994) 2961;
- (g) H. Nagao, T. Mizukawa, K. Tanaka, *Inorg. Chem.* 33 (1994) 3415;
- (h) S. Chardon-Noblat, M.N. Collomb-Dunand-Sauthier, A. Deronzier, R. Ziessel, D. Zsoldos, *Inorg. Chem.* 33 (1994) 4410;
- (i) S. Chardon-Noblat, A. Deronzier, R. Ziessel, D. Zsoldos, *Inorg. Chem.* 36 (1997) 5384;
- (j) T. Mizukawa, K. Tsuge, H. Nakajima, K. Tanaka, *Angew. Chem. Int. Ed.* 38 (1999) 362;
- (k) S. Rau, M. Ruben, T. Büttner, C. Temme, S. Dautz, H. Görls, M. Rudolph, D. Walther, A. Brodkorb, M. Duati, C. O'Connor, J.G. Vos, *J. Chem. Soc., Dalton Trans.* (2000) 3649;
- (l) K. Tanaka, T. Mizukawa, *Appl. Organomet. Chem.* 14 (2000) 863;
- (m) S. Chardon-Noblat, G.H. Cripps, A. Deronzier, J.S. Field, S. Gouws, R.J. Haines, F. Southway, *Organometallics* 20 (2001) 1668;
- (n) D. Ooyama, T. Kobayashi, K. Shiren, K. Tanaka, *J. Organomet. Chem.* 665 (2003) 107.
- [3] (a) M. Beley, J.-P. Collin, R. Louis, B. Metz, J.-P. Sauvage, *J. Am. Chem. Soc.* 113 (1991) 8521;
- (b) J.-P. Collin, M. Beley, J.-P. Sauvage, F. Barigelletti, *Inorg. Chim. Acta* 186 (1991) 91;
- (c) M. Beley, J.-P. Collin, J.-P. Sauvage, *Inorg. Chem.* 32 (1991) 4539;
- (d) M. Beley, S. Chodorowski, J.-P. Collin, J.-P. Sauvage, *Tetrahedron Lett.* 34 (1993) 2933;
- (e) M. Beley, S. Chodorowski, J.-P. Collin, J.-P. Sauvage, L. Flamigni, F. Barigelletti, *Inorg. Chem.* 33 (1994) 2543;
- (f) M. Beley, S. Chodorowski-Kimmes, J.-P. Collin, P. Lainé, J.-P. Launay, J.-P. Sauvage, *Angew. Chem., Int. Ed. Engl.* 33 (1994) 1775;
- (g) F. Barigelletti, L. Flamigni, M. Guardigli, A. Juris, M. Beley, S. Chodorowski-Kimmes, J.-P. Collin, J.-P. Sauvage, *Inorg. Chem.* 35 (1996) 136;
- (h) A. Jouaiti, M. Geoffroy, J.-P. Collin, *Inorg. Chim. Acta* 245 (1996) 69;
- (i) S. Chodorowski-Kimmes, M. Beley, J.-P. Collin, J.-P. Sauvage, *Tetrahedron Lett.* 37 (1996) 2963;
- (j) F. Barigelletti, L. Flamigni, J.-P. Collin, J.-P. Sauvage, *Chem. Commun.* (1997) 333;
- (k) J.-P. Collin, R. Kayhanian, J.-P. Sauvage, G. Calogero, F. Barigelletti, A. de Cian, F. Fischer, *Chem. Commun* (1997) 775;
- (l) C. Patoux, J.-P. Launay, M. Beley, S. Chodorowski-Kimmes, J.-P. Collin, S. James, J.-P. Sauvage, *J. Am. Chem. Soc.* 120 (1998) 3717;
- (m) A.-C. Laemmel, J.-P. Collin, J.-P. Sauvage, *Eur. J. Inorg. Chem.* (1999) 383;
- (n) J.-C. Roboin, M. Beley, G. Kirsch, *Tetrahedron Lett.* 41 (2000) 1175;
- (o) F. Barigelletti, B. Ventura, J.-P. Collin, R. Kayhanian, P. Gaviña, J.-P. Sauvage, *Eur. J. Inorg. Chem.* (2000) 113;
- (p) I.M. Dixon, J.-P. Collin, *J. Porphyrins, Phthalocyanines* 5 (2001) 600.
- [4] (a) E.C. Constable, M.J. Hannon, *Inorg. Chim. Acta* 211 (1993) 101;
- (b) E.C. Constable, A.M.W. Cargill Thompson, S. Greulich, *Chem. Commun.* (1993) 1444;
- (c) M.P. Ward, *J. Chem. Soc., Dalton Trans.* (1994) 3095;
- (d) E.C. Constable, A.M.W. Cargill Thompson, *Supramol. Chem.* 4 (1994) 95;
- (e) E.C. Constable, A.M.W. Cargill Thompson, J. Cherryman, T. Liddiment, *Inorg. Chim. Acta* 235 (1995) 165;
- (f) D.A. Bardwell, J.C. Jeffery, E. Schatz, E.E.M. Tilley, M.D. Ward, *J. Chem. Soc., Dalton Trans.* (1995) 825;
- (g) D.A. Bardwell, A.M.W. Cargill Thompson, J.C. Jeffery, J.A. McCleverty, M.D. Ward, *J. Chem. Soc., Dalton Trans.* (1996) 873;
- (h) A.M.W. Cargill Thompson, J.A. McCleverty, M.D. Ward, *Inorg. Chim. Acta* 250 (1996) 29;
- (i) E.C. Constable, A.M.W. Cargill Thompson, *New J. Chem.* 20 (1996) 65;
- (j) E.C. Constable, D.G.F. Rees, *New J. Chem.* 21 (1997) 369;
- (k) E.C. Constable, D.G.F. Rees, *Polyhedron* 17 (1998) 3281.
- [5] A. Mamo, I. Stefio, A. Poggi, C. Tringali, C. di Pirtro, S. Campagna, *New J. Chem.* 21 (1997) 1173.
- [6] M. Chavarot, Z. Pikramenou, *Tetrahedron Lett.* 40 (1999) 6845.
- [7] Y. Jahng, J.-G. Park, *Bull. Korean Chem. Soc.* 20 (1999) 1200.
- [8] C. Mikel, P.G. Potvin, *Inorg. Chim. Acta* 325 (2001) 1.
- [9] C. Bonnefous, A. Chouai, R.P. Thummel, *Inorg. Chem.* 40 (2001) 5851.
- [10] (a) T. Koizumi, T. Tomon, K. Tanaka, *Organometallics* 22 (2003) 970;
- (b) T. Koizumi, T. Tomon, K. Tanaka, *Bull. Chem. Soc. Jpn.* 76 (2003) 1969.
- [11] (a) K. Tanaka, Y. Kushi, K. Tsuge, K. Toyohara, T. Nishioka, K. Isobe, *Inorg. Chem.* 37 (1998) 120;
- (b) E. Simón-Manso, C.P. Kubiak, *Organometallics* 24 (2005) 231.
- [12] *International Tables for X-ray Crystallography*, vol. 4, Kynoch, Birmingham, England, 1974.
- [13] H. Nakajima, H. Nagao, K. Tanaka, *J. Chem. Soc., Dalton Trans.* (1996) 1405.
- [14] Still, coordination mode exchange of the napy ligand in **1** and **2** takes place easily. For instance, preliminary X-ray crystallographic data for **1** recrystallized from MeCN–Et₂O exhibits that the structure is [RuL¹(napy-κN)(NCMe)(dmsO)](PF₆)₂, where napy and DMSO are situated at mutually trans position. That is to say, the chelated napy ligand can dechelate by other coordinatable molecules.
- [15] (a) H. Nakajima, T. Mizukawa, H. Nagao, K. Tanaka, *Chem. Lett.* (1995) 251;
- (b) H. Nakajima, Y. Kushi, H. Nagao, K. Tanaka, *Organometallics* 14 (1995) 5093;
- (c) H. Sugimoto, K. Tanaka, *J. Organomet. Chem.* 622 (2001) 280.
- [16] We tried to synthesize the dicarbonyl complex, [Ru(N,N,C)-(napy-κN)(CO)₂]²⁺ by the reaction of complex **1** with CO (20 atm.) at 70 °C for 2 days in CH₃OCH₂CH₂OH. However, mixtures of mono- and di-carbonyl complexes ([Ru(N,N,C)-(napy-κ²N,N')(CO)]²⁺ and [Ru(N,N,C)(napy-κN)(CO)₂]²⁺) were produced in the reaction based on the ESI-MS spectra of the crude products. Several attempts to separate the mono- and dicarbonyl complexes were not succeeded. The mixture of those compounds showed ν(CO) bands at 2054, 2000, and 1990 cm⁻¹, which shifted to 1966, 1942, and 1880 cm⁻¹, respectively, upon the controlled potential electrolysis of the mixture at -1.45 V (vs. Fc/Fc⁺) in CD₃CN.